Two-dimensional clusters of liquid ^{4}He

A. Sarsa
Departmento de Física Moderna, Universidad de Granada, E-18071 Granada, Spain
and International School for Advanced Studies, SISSA, Via Beirut 2/4, I-34014, Trieste, Italy

J. Mur-Petit and A. Polls
Departament d'Estructura i Constituents de la Matèria, Universitat de Barcelona, Diagonal, 647, E-08028 Barcelona, Spain

J. Navarro
IFIC, CSIC-Universitat de València, Apartado 20285, E-46071 València, Spain

(Received 15 May 2003; revised manuscript received 7 October 2003; published 19 December 2003)

The binding energies of two-dimensional clusters (puddles) of ^{4}He are calculated in the framework of the diffusion Monte Carlo method. The results are well fitted by a mass formula in powers of $x=N^{-1/2}$, where N is the number of particles. The analysis of the mass formula allows for the extraction of the line tension, which turns out to be 0.121 K/Å. Sizes and density profiles of the puddles are also reported.

DOI: 10.1103/PhysRevB.68.224514 PACS number(s): 67.70.+n, 36.40.−c, 61.46.+w

I. INTRODUCTION

In recent years, a great deal of work has been devoted to studying quantum liquids in restricted geometries.[1] One important feature of these systems is that their internal structure becomes more easily observable than in bulk liquids due to the restricted motion of the particles in the confining potential. Among these systems the study of quantum films has received particular attention. They consist of liquid helium adsorbed to a more-or-less attractive flat surface. In 1973, Bretz *et al.*[2] observed the adsorption of ^{4}He onto the basal plane of graphite. In the last few years, adsorption properties of helium on different substrates such as carbon, alkali and alkaline-earth flat surfaces, carbon nanotubes, and aerogels have become a fertile topic of research.

The structure and growth of thin films of ^{4}He adsorbed to a substrate was studied by Clements *et al.*[3] employing the optimized hypernetted-chain Euler-Lagrange theory with realistic atom-atom interactions. It turns out that films with low surface coverages, where all atoms cover the surface with a thickness corresponding to a single atom, can be approximated reasonably well by a two-dimensional (2D) model. In connection with these systems, an interesting question naturally arises as how physics depends on the dimensionality of the space.

The homogeneous 2D liquid has been studied using different theoretical methods, such as molecular dynamics[4] and quantum Monte Carlo simulations with both Green's function[5] or diffusion[6] techniques. The inhomogeneous case was studied by Krishnamachari and Chester,[7] who used a shadow variational wave function to describe 2D puddles of liquid ^{4}He. In this work we report energies and density profiles of puddles calculated within the diffusion Monte Carlo (DMC) method. Our main objective is to give an accurate estimate of the line energy or the line tension of the 2D liquid ^{4}He. As atom-atom interactions we have used the revised version of the Aziz potential dubbed as HFD-B(HE).[8] This potential has been used to study ground-state properties of 3D bulk ^{4}He and ^{3}He,[9,10] within the DMC framework, and it has proved to accurately reproduce the ground-state properties of both liquids at zero temperature.

The trial wave function used for the importance sampling in the DMC calculation is introduced in Sec. II, where the variational Monte Carlo (VMC), results for this wave function are also reported. A brief explanation of the DMC techniques used in the present paper is presented in Sec. III. Section IV contains the DMC results and their analysis in terms of a mass formula in 2D. The line tension is extracted from this mass formula. Properties characterizing the puddles, such as the density profiles, are discussed in Sec. V. Finally, the main conclusions are summarized in Sec. VI.

II. VARIATIONAL GROUND-STATE ENERGIES

To study a system of N ^{4}He atoms in two dimensions we start from the following trial wave function:

$$\Phi_T(\mathbf{R})=\prod_{i<j}\exp\left[-\frac{1}{2}\left(\frac{b}{r_{ij}}\right)^{\nu}-\frac{\alpha^2}{2N}r_{ij}^2\right], \qquad (1)$$

written in the same way as in the 3D case.[11] The coordinate $\mathbf{R}$ indicates the set of coordinates of all the particles $\{\mathbf{r}_1,\mathbf{r}_2,\ldots,\mathbf{r}_N\}$, while r_{ij} stands for the interparticle distance, $r_{ij}=|\mathbf{r}_j-\mathbf{r}_i|$. The trial wave function contains the simple McMillan form[12] to deal with the very short-range part of the interaction and the translationally invariant part of a harmonic oscillator (HO) wave function with parameter α to roughly confine the system.

In our calculations the value $\hbar^2/m_4=12.1194$ K Å^2 has been employed for the atom mass and the parameters b and ν have been fixed to the values 3.00 Å and 5, respectively, the same values as in 3D calculations. The variational search has thus been restricted to the HO parameter α, whose optimal value is given in Table I. The expectation value of the Hamiltonian, as well as the separate contributions of kinetic and potential energies, are given in the same table for puddles with N atoms. It can be seen that the total energy results from an important cancellation between kinetic and potential en-

TABLE I. Variational results for the ground-state energy per particle E/N of 2D ^{4}He puddles of various cluster sizes. The confining HO parameter α is given in Å^{-1} and all energies are in K. The expectation values of the kinetic and the potential energies are also displayed. The column labeled KC refers to the VMC results of Ref. 7.

N	α	E/N	T/N	V/N	KC
8	0.1565	−0.2239(2)	1.3003(6)	−1.5242(5)	—
16	0.129	−0.3510(2)	1.7354(6)	−2.0864(5)	−0.380(8)
36	0.094	−0.4532(4)	2.031(3)	−2.484(3)	−0.471(7)
64	0.073	−0.4961(7)	2.159(2)	−2.655(2)	−0.528(5)
121	0.054	−0.5241(6)	2.223(2)	−2.747(2)	−0.570(7)
165	0.047	−0.5328(3)	2.289(1)	−2.822(1)	−0.602(7)
512	0.0266	−0.5493(5)	2.282(3)	−2.831(3)	−0.621(2)
∞	0.0000	−0.6904(8)	4.312(2)	−5.003(1)	—

ergies, which is in fact larger than in the 3D case. Let us recall that in 3D bulk, the energy per particle results from adding ≈ 14 K of kinetic energy with ≈ −21 K of potential energy. In 2D, both kinetic and potential contributions are very close to each other, which makes the calculation very delicate.

In the last column of Table I the VMC results of Krishnamachari and Chester[7] are reported. As compared with their results, our calculations provide smaller binding energies, in spite of the fact that the interaction used in Ref. 7 is an older version of the Aziz potential, which tends to underbind the systems. In fact, the shadow wave function used in Ref. 7 contains more elaborate correlations not present in our simple trial wave function. The VMC energy for the bulk system corresponds to the saturation density $\rho_0 = 0.04344$ Å^{-2}, taken from the DMC calculation of Ref. 6.

We have also performed calculations using a different trial wave function, replacing the translationally invariant Gaussian part by an exponential one—i.e.,

$$\Phi_T(\mathbf{R}) = \prod_{i<j} \exp\left[-\frac{1}{2}\left(\frac{b}{r_{ij}}\right)^{\nu} - \frac{\alpha}{2} r_{ij} \right], \tag{2}$$

expecting that this larger tail in the wave function will result in more binding. Actually, we do not find significant differences for small values of N. For instance, in the case $N=8$, using the same values for b and ν as before, we get $E/N = -0.2178(5)$ K, $T/N = 1.266(2)$ K, and $V/N = -1.484(2)$ K for $\alpha = 0.035$ Å^{-1}. When the values of b, ν and α are optimized, we obtain a slightly larger binding energy, $E/N = -0.2267(8)$ K for $b = 3.04$ Å, $\nu = 5.0$, and $\alpha = 0.035$ Å^{-1}. For greater values of N, the Gaussian *Ansatz* tends to provide more binding than the exponential. For example, with the exponential *Ansatz*, for $N=16$ we get $E/N = -0.1816(7)$ K for $\alpha = 0.023$ Å^{-1}, and optimizing the different parameters one gets $E/N = -0.2514(6)$ K, with $b = 3.04$ Å. In conclusion, the Gaussian wave function seems appropriate to be used as importance sampling in the DMC calculations.

III. DIFFUSION MONTE CARLO GROUND-STATE ENERGIES

Quantum Monte Carlo (QMC) methods provide the exact ground-state energy of a boson system, except for statistical errors. These techniques solve numerically the Schrödinger equation by means of a statistical simulation. They have been widely described in the literature; hence we briefly recall here the main ideas, referring the reader to, for example, Ref. 13 for a more detailed description on QMC techniques. In this work we use the DMC method to solve the Schrödinger equation in imaginary time ($\tau = it$) for the function

$$f(\mathbf{R},\tau) = \Phi_T(\mathbf{R})\Psi(\mathbf{R},\tau), \tag{3}$$

where $\mathbf{R}$ represents all the particle coordinates and is usually called "the walker," $\Psi(\mathbf{R},\tau)$ is the wave function of the system, and $\Phi_T(\mathbf{R})$ is the previously determined trial wave function (Sec. II), used here as importance sampling. It is convenient to write the solution of the time-dependent Schrödinger equation in the following form:

$$f(\mathbf{R},\tau+\Delta\tau) = \int d\mathbf{R}' G(\mathbf{R},\mathbf{R}',\Delta\tau) f(\mathbf{R}',\tau), \tag{4}$$

where G is the time-dependent Green's function and is formally written as

$$G(\mathbf{R},\mathbf{R}';\tau) = \langle \mathbf{R} | e^{-H\tau} | \mathbf{R}' \rangle, \tag{5}$$

where H is the Hamiltonian of the system. The function $G(\mathbf{R},\mathbf{R}';\tau)$ represents the amplitude probability for the transition from an initial state $\mathbf{R}'$ to a final one $\mathbf{R}$ in a time τ. In the limit $\tau \to \infty$, Eq. (4) gives the exact ground-state wave function. Thus, knowing G for infinitesimal time steps $\Delta\tau$, the asymptotic solution for large times $f(\mathbf{R},\tau\to\infty)$ can be obtained by solving iteratively the above equation. To this end, the exponential entering Eq. (5) is approximated to some fixed order in $\Delta\tau$. Both first- and second-order[9] propagators have been implemented in the present work and both of them provide the same extrapolated energy, within statistical errors, using the trial function Φ_T of Eq. (1) as guiding function. Our simulations have been carried out with a population of typically 400 walkers. As usual, some runs are first done to establish the asymptotic region of the short-time propagator; then several values of the time step have been used, and finally a fit, either linear or quadratic, has been carried out to obtain the extrapolated energy. For example, for $N=16$ the time steps 0.0001, 0.0002, 0.0003, and 0.0004 K^{-1} have been used to perform the extrapolation. In general, the statistical error is of the order of the time step error in our calculations.

In Table II we present the results of our linear DMC calculations of the total energy per particle for puddles containing N atoms. We have also reported and reproduced the results of the binding energy per particle of homogeneous 2D liquid ^{4}He at the equilibrium density $\rho_0^{DMC} = 0.04344(2)$ Å^{-2}, obtained in Ref. 6, where the same version of the Aziz potential was used. For this case, the simulations have been carried out for a system of 64 atoms with periodic boundary conditions, for which the errors due to

TABLE II. Energy per particle (in K) for 2D ^{4}He puddles for various cluster sizes obtained with the DMC algorithm.

N	8	16	36	64	121	∞
E/N	$-0.2613(4)$	$-0.4263(4)$	$-0.578(2)$	$-0.658(4)$	$-0.710(2)$	$-0.899(2)$

finite-size effects are smaller than the statistical ones.[5] We have also performed quadratic DMC calculations for some puddles and found results which are compatible with the linear DMC ones within their error bars. For example, the quadratic algorithm provides $E_{quad}=-0.2612(2)$ K for $N=8$ and $-0.652(4)$ for $N=64$. As expected, the DMC results lower the corresponding energies obtained by VMC either with our simple variational wave function or with a shadow wave function,[7] by up to $\sim 25\%$ in the case of the bulk system. It is worth mentioning that the final DMC result for the energy does not depend on the trial wave function for a boson system like the studied here, a fact that in the present case has been numerically checked for the Gaussian and the exponential *Ansätze*, Eqs. (1) and (2). Indeed, for boson systems the DMC method provides exact ground-state energies, within statistical errors.

IV. ENERGY AND LINE TENSION

For a saturating self-bound system, the ground-state energy per particle can be expanded in a series of powers of the variable $N^{-1/D}$, where N is the number of constituents and D is the dimensionality of the space. This is the well-known mass formula, which in the present case is written

$$E(N)/N=\varepsilon_b+\varepsilon_l x+\varepsilon_c x^2+\cdots, \tag{6}$$

with $x=N^{-1/2}$. The two first coefficients of this expansion are the bulk energy ε_b and the line energy ε_l, out of which the line tension λ is defined by $2\pi r_0\lambda=\varepsilon_l$. Here r_0 is the unit radius, defined as the radius of a disk whose surface is equal to the inverse of the equilibrium density of the 2D bulk liquid—i.e., $\rho_0\pi r_0^2=1$. Finally, ε_c is the so-called curvature energy.

Our calculated ground-state energies (Tables I and II) are plotted in Fig. 1 as a function of $N^{-1/2}$. One can see that the differences between our VMC and DMC energies increase with the number of atoms in the puddle. This clearly mirrors the simplicity of the trial wave function, which could be improved by including, for example, three-body correlations. Nevertheless, this trial function is adequate for the importance sampling in the DMC calculation.

We have fitted these energies to a parabolic mass formula like Eq. (6). The coefficients of the fit are given in Table III, together with the deduced line tension. Notice that the coefficient ε_b is identical, within statistical errors, to the bulk energy per particle of Table II. In fact, the χ^2 of the fit is very small, $\chi^2=5.7\times10^{-6}$. Regarding the line tension and despite using a different version of the Aziz potential and a different trial function, we notice that our VMC estimate is rather close to the one reported in Ref. 7, $\lambda=0.07$ K/Å. However, both VMC results are remarkably different from the DMC line tension, $\lambda=0.121$ K/Å.

To stress the curvature effect we have also plotted in the figure a straight line between the $N=8$ and bulk DMC values. A linear fit of the DMC energies gives coefficients $\varepsilon_b=-0.885$ K and $\varepsilon_l=1.80$ K, which are appreciably different from the previous ones. The bulk energy extrapolated from this linear fit differs from the directly calculated value, and the corresponding line energy is closer to the variational one, thus giving a bad estimation for the linear tension. In all cases, the line energy coefficient is approximately minus twice the volume energy term, similarly to the 3D case,[11] and

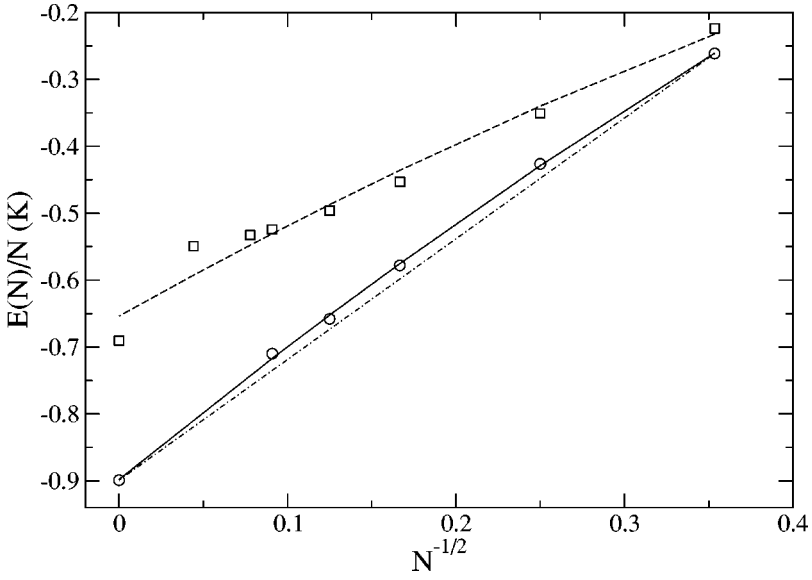

FIG. 1. Energies per particle (in K) of N-atom puddles as a function of $N^{-1/2}$, obtained from our VMC (squares) and DMC (circles) calculations. The interaction used is Aziz HFD-B(HE). Dashed and solid lines correspond to a least-squares fit to these energies. The dot-dashed line is a straight line between the $N=8$ and bulk DMC values.

TABLE III. Coefficients (in K) of a parabolic fit of the mass formula, as given in Eq. (6). The last column displays the deduced line tension (in K $Å^{-1}$).

	ε_b	ε_l	ε_c	λ
VMC	−0.654(1)	1.41(1)	−0.62(2)	0.083(1)
DMC	−0.898(2)	2.05(2)	−0.71(3)	0.121(1)

therefore one expects curvature effects to be important. In both VMC and DMC cases the extracted ε_c is negative—i.e., the binding energy is a convex function of x as it also happens for the 3D clusters.[11] This is in contrast with the value of ε_c reported in Ref. 7 which was positive but rather smaller than ours in absolute value and with larger error bars. Actually, as argued in Ref. 11 for 3D clusters, one would expect the curvature correction to the energy of a circular 2D cluster to be positive. Therefore, one should take the extracted value for ε_c with certain caution and not to emphasize its physical significance. However, it turns out that the value and sign of ε_c are stable against different possible fits—e.g., changing the number of points to build the fit or using a cubic mass formula. In any case the two first coefficients $\varepsilon_b, \varepsilon_l$ are quite robust against all performed fits. As an illustration, if one takes out the bulk point, the predicted bulk energy per particle and surface tension are equal to the reported ones within 1% and 5%, respectively. Therefore, the extracted line tension should be reliable, as also happens for 3D clusters.[11]

V. DENSITY PROFILES

The calculation of observables given by operators that do not commute with the Hamiltonian poses new problem to the DMC method. After convergence, the walkers are distributed according to the so-called mixed probability distribution given by the product of the exact and the trial wave functions. Therefore averaging the local values of the operator does not give the exact expectation value unless the operator commutes with the propagator. The result obtained by straightforward averaging is the mixed estimator which is correct up to first order in the trial wave function. Several options have been proposed in the literature in order to obtain unbiased (trial function independent and exact) values. In this work we have used the so-called *forward* or *future walking* technique[13] to calculate unbiased, also called pure, density profiles. The key ingredient to correct the mixed estimator is to include as a weight in the sampling the quotient $\Phi_{\text{exact}}(\mathbf{R})/\Phi_{\text{trial}}(\mathbf{R})$ for each walker, given by the asymptotic number of walkers. Several algorithms have been proposed in order to compute this quantity. In this work we use the algorithm developed in Ref. 14 that constitutes a simple and efficient implementation of the future walking method.

The pure DMC estimates of the density profiles for several puddles are plotted in Fig. 2. The figure also contains an horizontal line which indicates the saturation density (ρ_0^{DMC}) of the homogeneous system. For the puddle containing 36 atoms, the VMC profile obtained from a Gaussian *Ansatz* [Eq. (1)] is also shown for comparison as a dotted line. As one can appreciate in the figure, the process of optimization

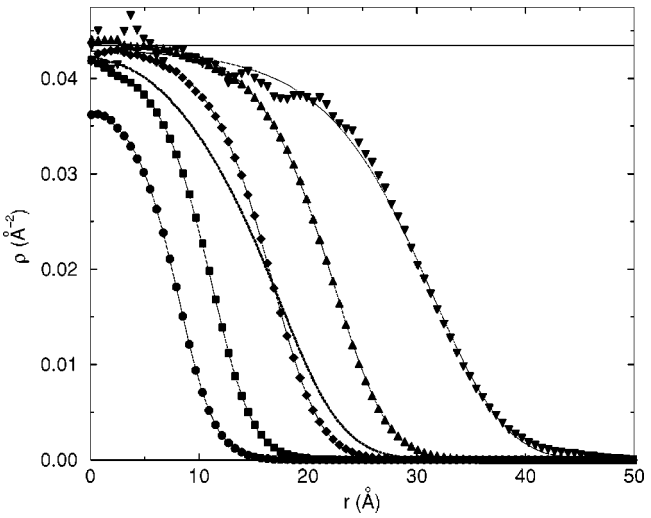

FIG. 2. Density profiles for ^{4}He puddles with various number of atoms, $N=8$ (circles), 16 (squares), 36 (diamonds), 64 (triangles up), and 121 (triangles down), obtained from our pure estimators for the linear DMC calculations. The solid horizontal line indicates the saturation density of the homogeneous system. The dotted line is the VMC profile for $N=36$ with a Gaussian trial function. The figure also contains the fits to the data provided by a generalized Fermi function, as explained in the text.

implied by the DMC method changes the profile reducing its thickness—i.e., producing a sharper surface. It can be seen that for the smaller clusters the central density is below ρ_0, while for the larger values of N shown in the figure the central density is above ρ_0, indicating a leptodermous behavior. One expects that, increasing the number of particles, the central density will approach ρ_0 from above, as in the 3D case.[15,16] It is worth noticing the oscillating behavior in the interior part of the density profile for $N=121$. It is difficult, however, to decide whether these oscillations are genuine or are simply due to a poor statistics in evaluating the pure estimator. Unfortunately, to discard this last option would require an exceedingly long computing time, within the scheme of this work.

The solid lines plotted in Fig. 2 are fits to our DMC densities provided by a generalized Fermi profile of the form

$$\rho(r)=\frac{\rho_f}{\left[1+\exp\left(\frac{r-R}{c}\right)\right]^{\nu}}. \tag{7}$$

The parameters defining the Fermi profile are given in Table IV together with the thickness t and the root-mean-square (rms) radius $\langle r^2\rangle^{1/2}$. We have checked that the rms radius calculated within the DMC code and the one derived form the fit agree to better than 0.5%, except for the $N=121$ case, where the difference is 1%. The rms radius grows with the number of particles as $N^{1/2}$, as expected. Therefore it grows faster than in 3D, in which case grows as $N^{1/3}$. This behavior allows for an alternative determination of the saturation density by performing a linear fit to the relation

TABLE IV. Parameters of a Fermi-profile fit to the density profiles. All lengths are in Å and ρ_f is in Å^{-2}. The parameter ν is adimensional.

N	ρ_f	R	c	ν	t	$\langle r^2\rangle^{1/2}$
8	0.03740	9.308	2.156	1.739	8.166	7.20
16	0.04204	13.38	2.656	2.284	9.580	9.18
36	0.04305	19.47	3.104	2.400	11.11	12.91
64	0.04386	26.68	3.783	3.111	13.09	16.68
121	0.04304	40.09	5.566	4.714	18.52	23.15

$$\langle r^2\rangle^{1/2} = \sqrt{\frac{N}{2\pi\rho_0}}. \tag{8}$$

The extracted value of ρ_0 from the mean-square radius reported in Table IV is 0.043 Å^{-2}, in good agreement with the determination from the calculation for the homogeneous system.

In the interval of N considered, the thickness t, defined as the distance over which the density falls from 0.9 of its value at origin to 0.1, is continuously increasing. However, as the finite value of the thickness for the semiinfinite system should define the asymptotic value of t, one expects that for larger puddles the thickness will probably have a maximum and smoothly approach this asymptotic value, as happens in the 3D case.[15] Finally, one also observes the asymmetric character of the density profiles with respect to the point at which the density falls at half its value at the origin. This can be appreciated by looking at the value of ν, which grows with N and also to the increasing difference between the quantities R and $\langle r^2\rangle^{1/2}$.

VI. SUMMARY AND CONCLUSIONS

In this work we have considered strictly two-dimensional systems of liquid ^{4}He, which are of course an idealization of a real quantum film. They are nevertheless interesting because their study can enlighten us as to the underlying structure of real quasi-2D systems. Of course, in the latter case, one has to take also into account the interaction with the substrate, which basically provides a global attractive potential. In the ideal 2D case, the suppression of the wave function component in the third dimension produces an increment of the global repulsion between atoms, resulting in a smaller binding energy per particle and a decrease of the equilibrium density.[17]

The binding energies of two-dimensional ^{4}He clusters, calculated by means of a diffusion Monte Carlo method, are well fitted by a mass formula in powers of $x=N^{-1/2}$. The analysis of the mass formula provides the main result of this paper—namely, the value of the line tension $\lambda = 0.121$ K/Å, which significantly differs from the one obtained from a similar analysis of VMC data and the one previously reported in the literature.[7] The quadratic term of the mass formula cannot be neglected and results in a negative value of the curvature energy as in the 3D case.[11,16] However, the studied clusters may be too small to give physical significance to this result.

The density profiles obtained with the pure estimator have been fitted by a generalized Fermi function, and the behavior of the rms radius and the thickness as well as the asymmetry character of the profile as a function of N has been discussed. However, calculations for larger puddles, which are out of the scope of the present paper due to limitations in computing time, would be necessary to describe the complete N dependence of the density profiles.

ACKNOWLEDGMENT

Fruitful discussions with X. Viñas are gratefully acknowledged. This work has been supported by DGICYT (Spain) Project No. PB98-1247, DGI (Spain) Grants Nos. BFM2001-0262 and BFM2002-00200, Generalitat de València grant GV01-216, Generalitat de Catalunya Project No. 2001SGR00064, and MURST (Italy) Grant No. MIUR-2001025498. J.M.P. acknowledges support from the Generalitat de Catalunya.

[1] See, e.g. *Microscopic Approaches to Quantum Liquids in Confined Geometries*, edited by E. Krotscheck and J. Navarro, Series on Advances in Quantum Many-Body Theory, Vol. 4 (World Scientific, Singapore, 2002).
[2] M. Bretz, J.G. Dash, D.C. Hickernell, E.O. McLean, and O.E. Vilches, Phys. Rev. A **8**, 1589 (1973).
[3] B.E. Clements, J.L. Epstein, E. Krotscheck, and M. Saarela, Phys. Rev. B **48**, 7450 (1993).
[4] C.E. Campbell and M. Schick, Phys. Rev. A **3**, 691 (1971).
[5] P.A. Whitlock, G.V. Chester, and M.H. Kalos, Phys. Rev. B **38**, 2418 (1988).
[6] S. Giorgini, J. Boronat, and J. Casulleras, Phys. Rev. B **54**, 6099 (1996).
[7] B. Krishnamachari and G.V. Chester, Phys. Rev. B **59**, 8852 (1999).
[8] R.A. Aziz, F.R. McCourt, and C.C.K. Wong, Mol. Phys. **61**, 1487 (1987).
[9] J. Boronat and J. Casulleras, Phys. Rev. B **49**, 8920 (1994).
[10] J. Casulleras and J. Boronat, Phys. Rev. Lett. **84**, 3121 (2000).
[11] V.R. Pandharipande, S.C. Pieper, and R.B. Wiringa, Phys. Rev. B **34**, 4571 (1986).
[12] W.L. McMillan, Phys. Rev. **138**, A442 (1965).
[13] B.L. Hammond, W.A. Lester, Jr., and P.J. Reynolds, *Monte Carlo Methods in ab initio Quantum Chemistry*, Lecture and Course Notes in Chemistry, Vol. 1 (World Scientific, Singapore, 1994).
[14] J. Casulleras and J. Boronat, Phys. Rev. B **52**, 3654 (1995).
[15] S. Stringari and J. Treiner, J. Chem. Phys. **87**, 5021 (1987).
[16] S.A. Chin and E. Krotscheck, Phys. Rev. B **45**, 852 (1992).
[17] See, e.g., V. Apaja and E. Krotscheck, in Ref. 1, Chap. 5, and references therein.